Whack-a-speckle: Focal Plane Wavefront Sensing in Theory and Practice with a Deformable Secondary Mirror and 5-micron Camera

Matthew A. Kenworthy, Philip M. Hinz, J. Roger P. Angel, Ari N. Heinze, Suresh Sivanandam

Steward Observatory, 933 North Cherry Avenue, Tucson, AZ 85721, USA

ABSTRACT

Long exposures from adaptive optic systems show a diffraction limited core superimposed on a halo of uncorrected light from a science target, and the addition of various long-lived speckles that arise from uncorrected aberrations in the telescope system. The presence of these speckles limit the detection of extra-solar planets at a few diffraction widths from the primary source. Focal plane wavefront sensing uses the deformable secondary mirror of the MMT adaptive optics system to systematically remove the presence of long-lived speckles in a high-contrast image, and also test for the incoherent source that represents a separate astronomical target nearby. We use the Clio 5 micron camera (with its coronagraphic capabilities) to modulate long lived speckles and present initial on-sky results of this technique.

Keywords: adaptive optics, wavefront sensing, mid infra-red

1. INTRODUCTION

In the past few years there has been a considerable effort to image planets around other stars, resulting in the first direct image of an exoplanet orbiting the brown dwarf 2M2107.[1] With the unique capabilities of the adaptive optics (AO) system on the 6.5 MMTO Telescope on Mount Hopkins at the University of Arizona, we are currently undertaking a mid-infrared survey to directly image extrasolar planet systems.[2]

The limiting factor for imaging exoplanet surveys with ground telescopes with AO correction (and likely also with TPF) is the presence of long-lived "speckles" which limit the imaging detection threshold.[3–5] We describe the technique of explicit speckle nulling to suppress these long-lived speckles. The technique relies on the fact that halo speckles which otherwise look like planets are coherent with the star. They can thus be removed ("whacked") by destructive interference with an "anti-speckle" created by appropriate modulation of a deformable mirror.

2. IMAGING EXTRA-SOLAR PLANETS AT 5 MICRONS

From a geometric consideration of the solid angle subtended by Jupiter as seen from the Sun, little more than 10^{-9} of the Sun's light is reflected from the planet's disk, and even at the relatively close distance of $5pc$, an extrasolar Jupiter would be just one arcsecond away from the parent star. The planet's signal is buried in the noise of the diffracted and scattered light of the primary star. Theoretical modeling of the spectra of extrasolar planets reveals that Jupiter and other giant planets glow in the thermal infrared due to the leftover heat from their formation.[6] Jupiter has a thermal radiation spectrum that peaks in the mid infrared, resulting in a planet to star flux ratio 100 to 1000 times larger than that in the visible.

Theoretical extrasolar giant planet (EGP) spectra produced by the Arizona group[7] show that for both isolated and irradiated exoplanets, the two atmospheric windows that show the most consistent planet to star flux ratio are the H and M bands (see Figure 1). It is important to note that these spectra are highly non-thermal, with the H and M bands sitting far above the equivalent blackbody spectrum. The relatively low sky background in the near infra-red, along with the higher spatial resolution and availability of AO corrected imaging has prompted

Further author information: (Send correspondence to M.A.K)
M.A.K: E-mail: mkenworthy@as.arizona.edu, Telephone: 1 520 626 6720

Advances in Adaptive Optics II, edited by Brent L. Ellerbroek, Domenico Bonaccini Calia,
Proc. of SPIE Vol. 6272, 62723B, (2006) · 0277-786X/06/$15 · doi: 10.1117/12.672577

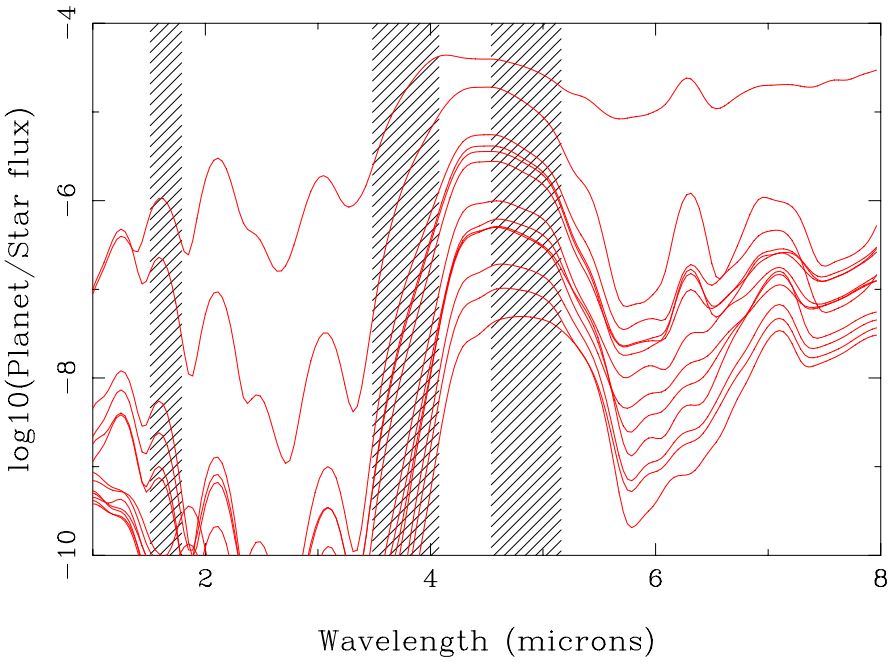

Figure 1. Theoretical contrast spectra of the 12 exoplanet candidates most suitable for direct imaging. H, L' and M bands are indicated in the shaded regions centered on 1.65, 3.78 and 4.85μm respectively. All spectra show the broad spectral feature at M band discussed in the text, from the massive EGP at the topmost curve (HD 39091b, $M \sin i$=10.3 M_{jup}), to the lowest mass planet at the bottom (47 UMa c, $M \sin i$=0.76 M_{jup}). Spectra are smoothed with a Gaussian filter of width 0.2μm

many groups to look for planets in the H band atmospheric window.[8,9] The broad 4-5 micron peak results from the combination of suppressed flux longward of 10 microns by collision-induced absorption of H_2 and windows in the H_2O opacity spectrum in the atmosphere of the EGP. These two effects force flux blueward, producing large flux enhancements over blackbody values in the J, H and M bands. As the planets cool, the M band stays brighter than both the J and H bands, and the Wien law blackbody quickly suppresses the bluer J and H band. As can be seen in Figure 1 the planet to star flux ratio is consistently brighter in M band for a whole range of planet models than the flux in H band.

3. THE MMT ADAPTIVE OPTICS SYSTEM AND CLIO CORONAGRAPHIC CAMERA

The 6.5m MMTO telescope is the first realization of a large aperture telescope coupled with a deformable secondary mirror that delivers an AO corrected $f/15$ beam (see Figure 2). Currently the system achieves typical Strehl ratios of 30-40% at H band (1.6μm) with a FWHM of 68 milliarcseconds. Measurements taken with the BLINC/MIRAC mid-IR camera in January 2003 recorded the first ever high Strehl AO images taken at 10μm. The Strehl ratio achieved was of order 96%.

At longer wavelengths ($> 2.5\mu m$) the MMT AO system is uniquely sensitive because of the lower background light it emits at infrared wavelengths compared to conventional AO systems. This is because it uses a deformable secondary mirror for wavefront correction[10] which has the advantage of eliminating approximately 8 warm, dusty, optical surfaces from the typical AO system design.[11] The elimination of these extra optical surfaces (that are required for conventional large telescope AO systems e.g., Keck, VLT, etc.) allows the MMT AO to have much lower scattered light and lower thermal emissivity, whilst increasing the system throughput. Conservative estimates of this suggest that 6.5 m MMT AO system in conventional imaging mode will be as efficient as the 10 m Keck AO system at H (1.6μm) and 2.28 times as efficient at N (10.5μm) despite having a smaller primary mirror.[12] We have measured the emissivity of the MMT system to be approximately 7% in thermal infrared

Figure 2. The MMT AO System. The successive pictures show the 6.5m MMTO telescope, the deformable secondary mirror in the telescope hub, and a detail of the secondary mirror during assembly in the optics laboratory showing the location of the 336 mirror actuators.

observations. This is already much improved over the 20% emissivity expected of conventional AO systems. Where telescope background is the dominant source of background photons (as it is for the most transparent portions of the L band and portions of the M band atmospheric window), a reduction in emissivity corresponds to a direct reduction in exposure time to reach a particular sensitivity.

Our optimized 3-5 micron imager and coronagraph, named Clio,[2] has been completed and is currently being used for scientific observations at the MMTO. The Clio camera consists of a $5\mu m$ camera that is optimised to work with diffraction limited images in H, L' and M bands. There are three channels that image at $f/20$, $f/35$ and a pupil imaging mode. The $f/20$ imaging mode is optimised to work in the high background regime of L' and M bands with Nyquist sampling at L' band (0.048"/pixel) and a field of view of 15" by 12".

Diffraction can be handled in several ways and we are exploring whether conventional coronagraphs,[13] band-limited masks,[14] or phase-induced suppression[15,16] will be most suitable. Diffracted light will need to be reduced to well below the level of the residual speckle halo in order to not add additional noise due to coherent combination with the speckles. For the level of the halo we expect using the MMT AO system at M band this corresponds to a suppression factor of 10-30 for the diffracted light. This is likely achievable with a standard Lyot coronagraph with a $4-5\lambda/D$ spot and a 10% undersized pupil stop or similar equivalent.

Recently we have developed an apodized plate design[17–19] that suppresses diffraction in a D-shaped region around the target star, by use of a transmitting optic of variable thickness at the pupil plane in the coronagraph. This modifies the wavefront so as to suppress Airy rings over one half of any point-like source, and results in a measured suppression[20] of 10 to 50 of the diffraction pattern. The advantages of this design over more traditional Lyot coronagraphs includes higher throughput efficiency and a complete insensitivity to telescope tracking and pointing errors.

Near infra-red observations with AO systems reveal speckle noise that limits the detection of planets with infra-red cameras.[5,8,9] A short exposure image from an AO corrected telescope shows the Airy diffraction pattern surrounded by a cloud of rapidly changing speckles, which are due to residual uncorrected wavefront errors in the AO system. As the integration time is increased, most speckles average out to produce a smooth "halo" of light that surrounds this diffraction limited core. However, in practice some speckles persist. These static speckles result from non common optical path errors between the science camera and the wavefront sensor camera that measures the incoming wavefront. This is a problem common to all high contrast imaging systems where the wavefront measurement path is not identical to the science camera path, and this has been observed on space telescopes such as the HST.[21] The dominant source of noise is then expected to be the ability to calibrate or suppress the persistent speckles. The high Strehl images delivered in L' and M bands (80% and 90% from current MMT AO performance) will create speckles which are expected to be symmetric if caused by path length rather than diffraction errors. To the degree this symmetry is preserved it can be used to subtract off long-lived speckles, however flat fielding and registration errors will ultimately limit this subtraction.

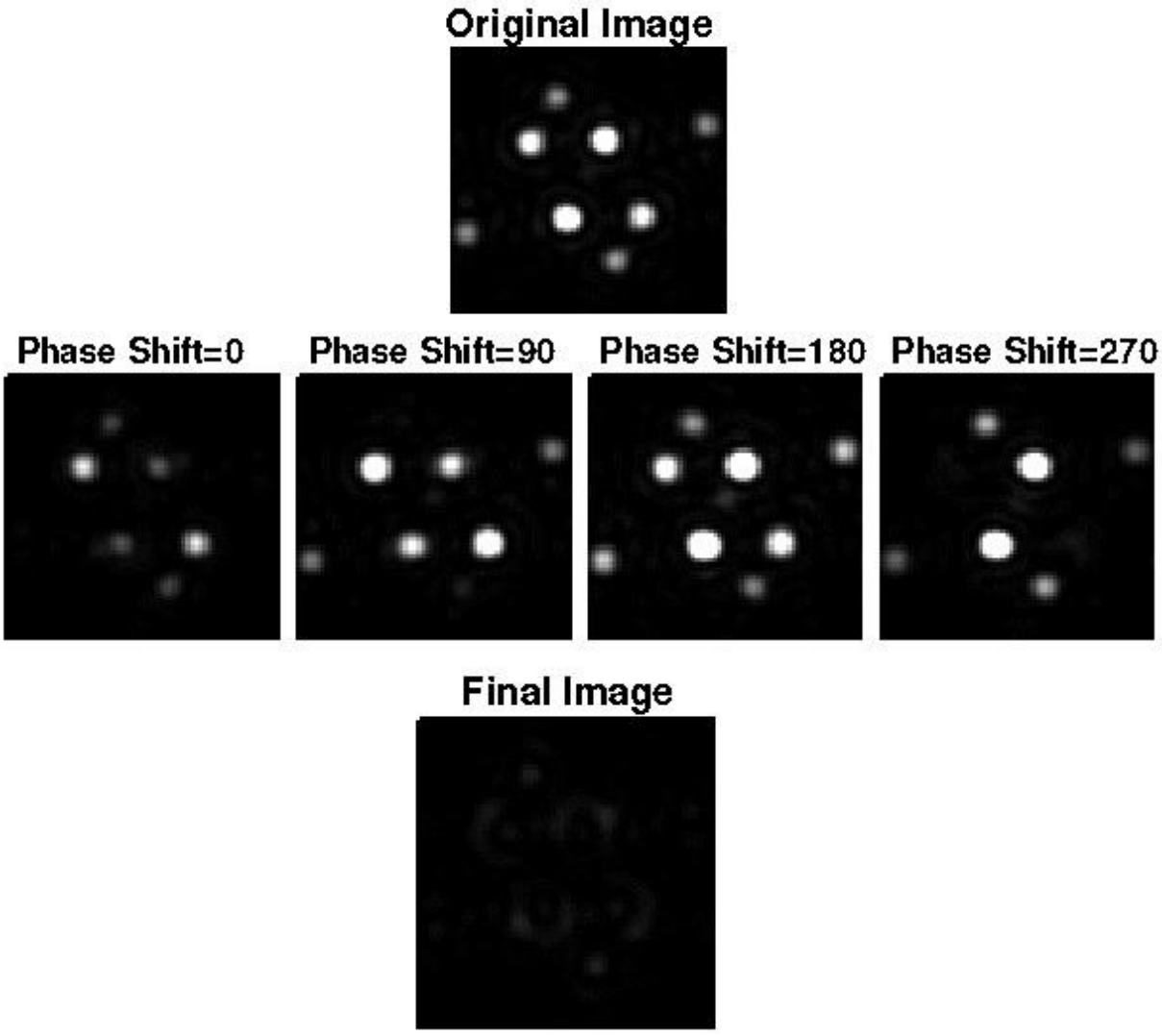

Figure 3. Simulation of focal plane wavefront sensing. The top image shows four speckles with various brightnesses. Four trial wavefronts are created and added to original wavefront, which modulated the brightness of each speckle. The phase of each speckle can be derived from these four intermediate images allowing application of a final corrected wavefront correction to the original which suppresses the original pattern by a factor of 20.

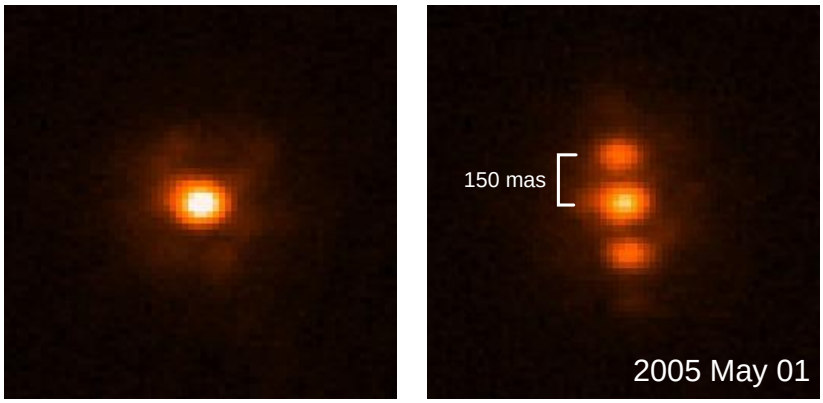

Figure 4. The first realisation of artificially generated speckles using the MMT deformable secondary mirror. These images are taken in H band using the ARIES camera, consisting of 10 x 1sec exposures co-added. The left hand image shows the closed loop PSF for the AO system, whilst the right hand image has a static sinusoidal wave of 150 nm r.m.s. with three cycles across the deformable mirror in addition to the AO wavefront corrections.

4. FOCAL PLANE WAVEFRONT SENSING THEORY AND INITIAL TESTS

The approach to implementing focal plane wavefront sensing we use is illustrated in Figure 3. After suppressing diffraction through a coronagraph, quasi-static speckles will be left at various points in the focal plane. Each speckle in the focal plane corresponds to a sinusoidal component of phase aberration in the pupil plane. The brightness of a speckle, its distance from the center of the star image, and its orientation determines the amplitude of the modulation, the spatial frequency of the wave, and its orientation in the pupil. The only missing information is the phase shift of the wave. To find this out we divide one side of the image into approximately λ/D regions and sum the corresponding sine waves to add to the original wavefront. The sum of all the waves is added to the original for sine waves which are shifted by 0, 90, 180, and 270 degrees. The phase for each λ/D region in the focal plane is then derived and a final corrected wavefront is generated which suppresses the original speckle pattern. Figure 3 shows that the resultant image after carrying out such a procedure efficiently removes the original pattern, reducing the maximum speckle in the example by a factor of 20.

The useful region of operation for focal plane wavefront sensing for the MMT AO and Clio is from approximately $3\lambda/D$, where we expect diffraction to be suppressed, out to approximately $9\lambda/D$ which is the maximum control radius for the 336 actuator MMT deformable mirror. This is 0.36-1.1" for L' and 0.48-1.4" for M band.

Our approach to suppressing the speckles will likely evolve as we develop experience with how long-lived the pattern is, as well as how good of a signal-to-noise we need to effectively reduce a peak. Currently we envision that initial images will show static speckles in relatively short (1-3 min.) integration times. We will then cycle through four phases of measurement to reduce the speckles to a level where they are not detectable until longer integrations have been achieved. By cycling through a four-phased measurement again we expect to reduce the static speckles to a level where we are unable to detect the pattern in even in our longest observing sequence. It is important to note that since a planet's light is not coherent, its light cannot be suppressed.

Figure 4 shows the **first on sky demonstration** taken with the 6.5m MMT and ARIES near infrared imaging camera[22] where we applied a fixed sinusoidal shape on the AO deformable mirror in closed loop operation to generate artifical speckles. By using a superposition of much smaller Fourier terms on the mirror, we can add and move weak speckles in the focal plane to destructively interfere with speckles produced by non-common path errors.

The extension of sensitivity for giant planets into 0.4" will allow searches for planets in the potentially fruitful range of 4-20 AU for typical stars at 7-20pc. These may both be more numerous, compared to 20-50 AU and more important for determining a star's suitability for having a stable habitable zone.

ACKNOWLEDGMENTS

Observations reported here were obtained at the MMT Observatory, a joint facility of the University of Arizona and the Smithsonian Institution.

REFERENCES

1. G. Chauvin, A.-M. Lagrange, C. Dumas, B. Zuckerman, D. Mouillet, I. Song, J.-L. Beuzit, and P. Lowrance, "Giant planet companion to 2MASSW J1207334-393254," A&A **438**, pp. L25–L28, Aug. 2005.
2. M. Freed, P. M. Hinz, M. R. Meyer, N. M. Milton, and M. Lloyd-Hart, "Clio: a 5-μm camera for the detection of giant exoplanets," in *Ground-based Instrumentation for Astronomy*, A. F. M. Moorwood and M. Iye, eds., *Proc. SPIE* **5492**, pp. 1561–1571, Sept. 2004.
3. R. Lenzen, L. Close, W. Brandner, B. Biller, and M. Hartung, "A novel simultaneous differential imager for the direct imaging of giant planets," in *Ground-based Instrumentation for Astronomy*, A. F. M. Moorwood and M. Iye, eds., *Proc. SPIE* **5492**, pp. 970–977, Sept. 2004.
4. A. Sivaramakrishnan, J. P. Lloyd, P. E. Hodge, and B. A. Macintosh, "Speckle Decorrelation and Dynamic Range in Speckle Noise-limited Imaging," ApJ **581**, pp. L59–L62, Dec. 2002.
5. R. Racine, G. A. H. Walker, D. Nadeau, R. Doyon, and C. Marois, "Speckle Noise and the Detection of Faint Companions," PASP **111**, pp. 587–594, May 1999.
6. A. Burrows, M. Marley, W. B. Hubbard, J. I. Lunine, T. Guillot, D. Saumon, R. Freedman, D. Sudarsky, and C. Sharp, "A Nongray Theory of Extrasolar Giant Planets and Brown Dwarfs," ApJ **491**, pp. 856–+, Dec. 1997.
7. A. Burrows, D. Sudarsky, and I. Hubeny, "Spectra and Diagnostics for the Direct Detection of Wide-Separation Extrasolar Giant Planets," ApJ **609**, pp. 407–416, July 2004.
8. B. A. Biller, L. Close, R. Lenzen, W. Brandner, D. W. McCarthy, E. Nielsen, and M. Hartung, "Suppressing speckle noise for simultaneous differential extrasolar planet imaging (SDI) at the VLT and MMT," in *Advancements in Adaptive Optics.*, D. Bonaccini Calia, B. L. Ellerbroek, and R. Ragazzoni, eds., *Proc. SPIE* **5490**, pp. 389–397, Oct. 2004.
9. B. R. Oppenheimer, A. P. Digby, L. Newburgh, D. Brenner, M. Shara, J. Mey, C. Mandeville, R. B. Makidon, A. Sivaramakrishnan, R. Soummer, J. R. Graham, P. Kalas, M. D. Perrin, L. C. Roberts, J. R. Kuhn, K. Whitman, and J. P. Lloyd, "The Lyot project: toward exoplanet imaging and spectroscopy," in *Advancements in Adaptive Optics*, D. Bonaccini Calia, B. L. Ellerbroek, and R. Ragazzoni, eds., *Proc. SPIE* **5490**, pp. 433–442, Oct. 2004.
10. G. Brusa, A. Riccardi, V. Biliotti, C. del Vecchio, P. Salinari, P. Stefanini, P. Mantegazza, R. Biasi, M. Andrighettoni, C. Franchini, and D. Gallieni, "Adaptive secondary mirror for the 6.5-m conversion of the Multiple Mirror Telescope: first laboratory testing results," in *Adaptive Optics Systems and Technology*, R. K. Tyson and R. Q. Fugate, eds., *Proc. SPIE* **3762**, pp. 38–49, Sept. 1999.
11. M. Lloyd-Hart, F. P. Wildi, B. Martin, P. C. McGuire, M. A. Kenworthy, R. L. Johnson, B. C. Fitz-Patrick, G. Z. Angeli, S. M. Miller, and J. R. P. Angel, "Adaptive optics for the 6.5-m MMT," in *Adaptive Optical Systems Technology*, P. L. Wizinowich, ed., *Proc. SPIE* **4007**, pp. 167–174, July 2000.
12. M. Lloyd-Hart, "Thermal Performance Enhancement of Adaptive Optics by Use of a Deformable Secondary Mirror," PASP **112**, pp. 264–272, Feb. 2000.
13. R. Gonsalves and P. Nisenson, "Calculation of Optimized Apodizers for a Terrestrial Planet Finder Coronagraphic Telescope," PASP **115**, pp. 706–711, June 2003.
14. M. J. Kuchner and D. N. Spergel, "Notch-Filter Masks: Practical Image Masks for Planet-finding Coronagraphs," ApJ **594**, pp. 617–626, Sept. 2003.
15. J. L. Codona and R. Angel, "Imaging Extrasolar Planets by Stellar Halo Suppression in Separately Corrected Color Bands," ApJ **604**, pp. L117–L120, Apr. 2004.
16. O. Guyon, "Phase-induced amplitude apodization of telescope pupils for extrasolar terrestrial planet imaging," A&A **404**, pp. 379–387, June 2003.
17. J. L. Codona, R. Angel, and N. Putnam, "Closed-loop halo suppression with an interferometric coronagraph," ApJ **in preparation**, 2006.

18. J. L. Codona, "Phase Apodization Coronagraphy," ApJ **in preparation**, 2006.
19. J. L. Codona, P. M. Hinz, M. A. Kenworthy, J. R. P. Angel, and N. J. Woolf, "High-contrast phase apodization at the MMT: design and on-sky tests," in *Ground-based and Airborne Instrumentation for Astronomy*, I. S. McLean and M. Iye, eds., *Proc. SPIE* **6269**, 2006.
20. M. A. Kenworthy, J. L. Codona, P. M. Hinz, and J. R. P. Angel, "First On-Sky Imaging with an Apodised Phase Plate," ApJ **in preparation**, 2006.
21. G. Schneider, E. Becklin, L. Close, D. Figer, J. Lloyd, B. Macintosh, D. Hines, C. Max, D. Potter, M. Rieke, N. Scoville, R. Thompson, A. Weinberger, and R. Windhorst, "Domains of Observability in the Near Infrared with HST/NICMOS and (Adaptive Optics Augmented) Large Ground Based Telescopes, solicited by STScI in preparation for HST Cycle 12, 2003," tech. rep., STScI, 2002.
22. D. W. McCarthy, J. H. Burge, J. R. P. Angel, J. Ge, R. J. Sarlot, B. C. Fitz-Patrick, and J. L. Hinz, "ARIES: Arizona infrared imager and echelle spectrograph," in *Infrared Astronomical Instrumentation*, A. M. Fowler, ed., *Proc. SPIE* **3354**, pp. 750–754, Aug. 1998.